Received: 8 January 2018 | Accepted: 22 July 2018

DOI: 10.1002/adv.22125

RESEARCH ARTICLE

WILEY

Characterization of polyamide 6.10 composites incorporated with microcrystalline cellulose fiber: Effects of fiber loading and impact modifier

Mohammad Dalour Hossen Beg[1] | **Muhammad Remanul Islam**[2] | **Abdullah Al Mamun**[3] | **Hans-Peter Heim**[3] | **Maik Feldmann**[3] | **John Olabode Akindoyo**[1]

[1]Faculty of Chemical and Natural Resources Engineering, Universiti Malaysia Pahang, Gambang, Pahang, Malaysia

[2]Malaysian Institute of Chemical and Bioengineering Technology, University of Kuala Lumpur, Bandar Alor Gajah, Melaka, Malaysia

[3]Institute of Materials Engineering, University of Kassel, Kassel, Germany

Correspondence
Mohammad Dalour Hossen Beg, Faculty of Chemical and Natural Resources Engineering, Universiti Malaysia Pahang, Leburaya Tun Razak, Gambang 26300, Pahang, Malaysia.
Email: dhbeg@yahoo.com
and
Muhammad Remanul Islam, Malaysian Institute of Chemical and Bioengineering Technology, University of Kuala Lumpur, Bandar Alor Gajah 78000, Melaka, Malaysia.
Email: muhammad.remanul@unikl.edu.my

Funding information
Hessisches Ministerium für Wissenschaft und Kunst

Abstract

Microcrystalline cellulose (MCC) fiber-reinforced polyamide 6.10 (PA) composites were prepared in the presence of an impact modifier (IM), exxelor VA1803 (VA), by melt compounding process. Fiber loading was considered from 20 to 30 wt.%, whereas IM was varied from 2.0 to 5.0 wt.%. Composites were characterized by tensile test, impact test, dynamic thermal mechanical analysis (DTMA), differential scanning calorimetry (DSC), thermogravimetric analysis (TGA), and X-ray diffraction (XRD). Composites' fractured surfaces were examined by scanning electron microscope (SEM). In addition, fiber size distribution was also analyzed. Result analyses showed that the fiber incorporation changed the tensile strength (TS) slightly, but the tensile modulus (TM) significantly. The TM was found to be improved by 45% at the amount of fiber loading of 30 wt.%. Moreover, the thermomechanical properties revealed that the storage modulus (SM) and loss modulus (LM) were increased due to the incorporation of MCC, which was improved further by the uses of 5.0 wt.% of VA. The MCC possess high crystallinity index and high crystallite size along with enhanced mechanical and thermal properties. Therefore, the extraordinary benefit of using MCC in PA was evaluated in terms of thermomechanical, structural, and thermal properties in the presence of the impact modifier.

KEYWORDS

coupling agent, microcrystalline cellulose (MCC), polyamide composite, thermomechanical

1 | INTRODUCTION

A number of polymers have been used for the preparation of composites for different selective purposes. Among them, petroleum and bio-based polymers are mentionable. Polyamide, an important polymer matrix for composites, can be obtained from petroleum and bio-based resources. Different kinds of polyamides are available depending on their structural differences. They have potential application in the field of thin-film membrane and composites.[1,2] Recently, polyamides have attracted interest by the manufacturer for some useful applications including electronics, buildings, engineering parts, sporting goods, automotive, housing, packaging, and consumer goods. Among the polyamides, PA 6 and PA 6.6 possess high mechanical strength, excellent ductility, and good resistivity to chemicals and heat exposure which are almost similar to PA 6.10, with some other additional benefits. In contrast, polyamide PA 11 has some limitations, for example, lower melting temperature and thermomechanical properties compared to the petroleum-based one. Therefore, the improvement of their properties is essential. For the

TABLE 1 The samples' code and their respective formulation

Samples' code	PA (wt.%)	Fiber (wt.%)	VA (wt.%)
PA	100	–	–
PA20F	80	20	–
PA30F	70	30	–
PA30F2VA	70	30	2.0
PA30F5VA	70	30	5.0

improvement, uses of different kinds of fillers and blending of PA with other type of polymers have been investigated.[3–5]

Different kinds of fillers, such as calcium carbonate, silica, mica, talc, carbon fiber, and glass fiber, have been used with polyamides to improve different properties. Recently, renewable and low-cost natural fibers (NFs) have been studied as fillers or reinforcing agent with the polyamides to improve the mechanical, thermal, and morphological properties. The NFs are cellulosic materials and exhibit very good performances as reinforcing agent to the polymer matrices.[6] While using NFs for the reinforcement with thermoplastics, such as polyethylene terephthalate and nylon, the processing temperature is a vital concern because of lower thermal stability of the NFs.[7–9] Therefore, polymers having melting point, below or around 200°C, can be used mostly for the preparation of NFs-based composites.[10,11] The purified cellulose fiber has higher thermal stability than NF and can be sustained up to the temperature of 250°C.[7–9] Compare to the purified cellulose fiber, NFs contain moisture, hemicellulose, and lignin. Therefore, in terms of thermal stability, the NFs start degrading around 100°C due to the loss of moisture, celluloses start degrading entirely from 250 to 350°C, whereas hemicelluloses start decomposing at 180–280°C. Moreover, they start decomposing at higher temperature (350–450°C) for long period due to the complex nature and big molecular size of the lignin. Reinforcement of cellulose in the polymer matrix was found to improve the Young's modulus of PLA-based composite in a previous study.[12] These fibers were also used for the preparation of PA 6 and PA 6.10-based composites.[13] A comparison was drawn among the mechanical properties, on the basis of the processing parameters of the composites. Result analyses revealed that the processing parameters have significant effects on the properties of the composites.[13,14]

The microcrystalline cellulose (MCC) fibers are important materials for pharmaceutical, food, paper, and composite industries. These materials are thermally stable up to 300°C and commercially available at lower price than synthetic fibers. These fibers have been used successfully with polystyrene and polyethylene to prepare composites.[15–17] They are potential reinforcing agent for polymer composites due to their high crystallinity index, high crystallite size, and excellent thermomechanical properties. On the other hand, ethylene copolymer grafted with maleic anhydride is especially manufactured for the improvement of impact properties of polyamides. Therefore, the main objective of this study was to find the effect of loading of microcrystalline cellulose fiber into polyamide 6.10 (PA), in the presence of exxelor VA1803 (VA), in terms of mechanical, thermal, structural, and thermomechanical properties. It is known that the polymer-based composites undergo degradation during the manufacturing process of melt casting. Therefore, it is important to analyze the influence of the processing temperatures during the fabrication of cellulose fiber-based polymer composites.

2 | MATERIALS AND METHODS

2.1 | Materials

In this research, polyamide 6.10 (PA) was used as polymer matrix. An amorphous ethylene copolymer, exxelor VA1803 (VA), functionalized with maleic anhydride, was used as impact modifier. Microcrystalline cellulose (MCC) fiber, FD600/30, Rettenmeier, Germany, was used for the reinforcement. The used MCC was white in color and in the form of powder. It was a native cellulose fiber, processed from the softwood, and usually, used for the technical application. The mean fiber length and mean fiber diameter were 45 and 25 μm, respectively. The bulk density of the fiber was 222 g/L. The chemical composition of the fibers was as follows: alpha cellulose of 73.1%, hemicellulose of 9.1%, and lignin of 7.2%.

2.2 | Fiber size distribution

The fiber size distribution was analyzed using a dynamic image analyzer (QICPIC) (Sympatec), with a wet dispersing unit, MIXCEL. Nearly, 2573K particles were analyzed in isopropanol, with an image resolution of 4.2 MP.

2.3 | Preparation of the composites

The composites were prepared using extrusion followed by injection molding. The PA and VA were dried (moisture content less than 0.1 wt.%) using an air dryer (TORO-systems TR–Dry–Jet EASY 15). The MCC was dried (moisture content less than 1.0 wt.%) in an oven before the extrusion process. The amount of the components of the composites for different formulation is presented in Table 1. The ingredients were extruded using a twin-screw extruder (model: ZSE 18 HPE, Leistritz), at 240°C (screw diameter: 18 mm, screw speed: 200 RPM, and process length: 40 D). The extruded samples were pelletized using a pelletizer (Scheer SGS 25-E), to a pellet size of 3 mm. The pelletized samples were

processed with an injection molding machine (Klöckner Ferromatik FM85).

2.4 | Tensile testing

The tensile testing was carried out according to the EN ISO 527 method, using a Zwick Z 010 testing machine, with a cross-head speed of 5 mm/min. The capacity of the load cell was 50 kN. Seven specimens were tested, and an average of the results was considered for the analysis. The Young's modulus, tensile strength, and elongation at break (%) of the composites were evaluated.

2.5 | Impact testing

Instrumented notched Charpy impact testing was carried out according to the EN ISO 179-2 method. The specimens were notched using a CEAST notching machine. The impact strength (IS) was determined using an instrumented Charpy impact pendulum (Zwick). Eight specimens were tested, and an average value of the results was considered for the impact strength.

2.6 | Dynamic thermomechanical analysis (DTMA)

The DTMA testing was conducted using a dynamical mechanical analyzer, DMA 2980/Q800, TA Instruments, according to DIN EN ISO 75-2:2013. The samples were analyzed in dual cantilever clamped bending mode. The measurements were performed in different temperature ranges (0–150°C). The testing was conducted over a wide range of frequency (1, 3, 10 Hz), with a constant heating rate (3°C/min) and a constant oscillating amplitude.

2.7 | Scanning electron microscopy (SEM)

The surface morphology of the fractured samples of the composites was examined using a scanning electron microscope, Zeiss Ultra 55 plus. The fractured notched Charpy specimens were coated with gold, and images were captured with a low level of magnification to obtain an overview of the fiber distribution and the fiber pull-outs. Images with a higher magnification were selected for the analysis.

2.8 | X-ray diffraction analysis

The structural property of the samples was measured by X-ray diffraction (XRD) analysis. For this purpose, A Rigaku Mini Flex II, Japan, was used with tube current of 15 mA and operating voltage of 30 kV. The samples were scanned stepwise from 5° to 40° of scattering angle (2θ), using Cu K_α radiation wavelength of λ1.541 Å.

2.9 | Thermogravimetric analysis

A thermogravimetric analyzer, TA Instrument (model-TA-Q500), was used to determine the thermal decomposition behavior of the composites. Nearly, 5 mg of the sample was considered in a platinum pan for the testing. The heating rate was 20°C/min for the temperature range of 30–600°C.

2.10 | Differential scanning calorimetry

For the melting behavior, a differential scanning calorimeter, TA Instrument (model-TA-Q1000), was used in nitrogen atmosphere. An aluminum pan was used for the testing with heating rate of 10°C/min and temperature range of 30–410°C. The percentage of crystallinity (X_{dsc}) was obtained using the following equation:[18,19]

$$X_{dsc} = \frac{\Delta H}{\Delta H_m W} \times 100\%$$

where ΔH is the heat of fusion of sample, ΔH_m represents the heat of fusion for 100% crystalline PA, and W is the mass fraction of the matrix. The heat of fusion was considered 190 J/g for the 100% crystalline polyamide.[20]

3 | RESULTS AND DISCUSSION

3.1 | Fiber size distribution and surface morphology

The fiber size and distribution have strong effects on the performance of composites. This is important to measure based on different manufacturing processes. The breakage of the fibers usually occurs during the processing (extrusion and injection molding) of composites.[21] The ultimate length of the fibers depends on their initial length, intercollision among the fibers, and between fibers and polymer. The distribution of the fiber size is presented in Figure 1. The figure showed a wide distribution according to different length of the fibers, and it was observed that the size of MCC was in a range of 3–20 μm. Almost 80% of the fiber length was in the range of 5–12 μm. No or very little fibers were observed less than 3 and more than 100 μm of size. It seems that a usual decay of the size distribution, with a peak of the length ranging from 5 to 12 μm. The interval for the numbers of fibers was adequate to get a fine distribution which ultimately reduces the volume fraction of matrix. It is noteworthy to mention that too small particle size is an easy mean of debonding subsequently can cause no matrix yielding for stress or load dissipation. Toughness of the formulated composites depends on the particle size distribution.[22] As PA is a brittle matrix, its toughness

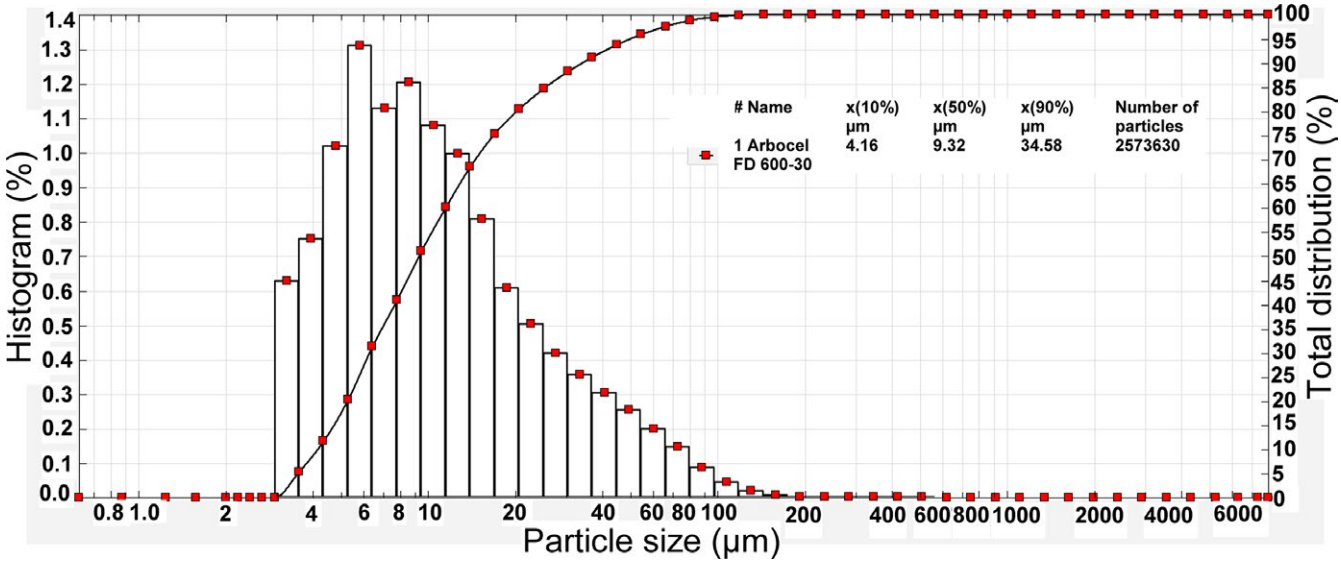

FIGURE 1 Fiber size distribution

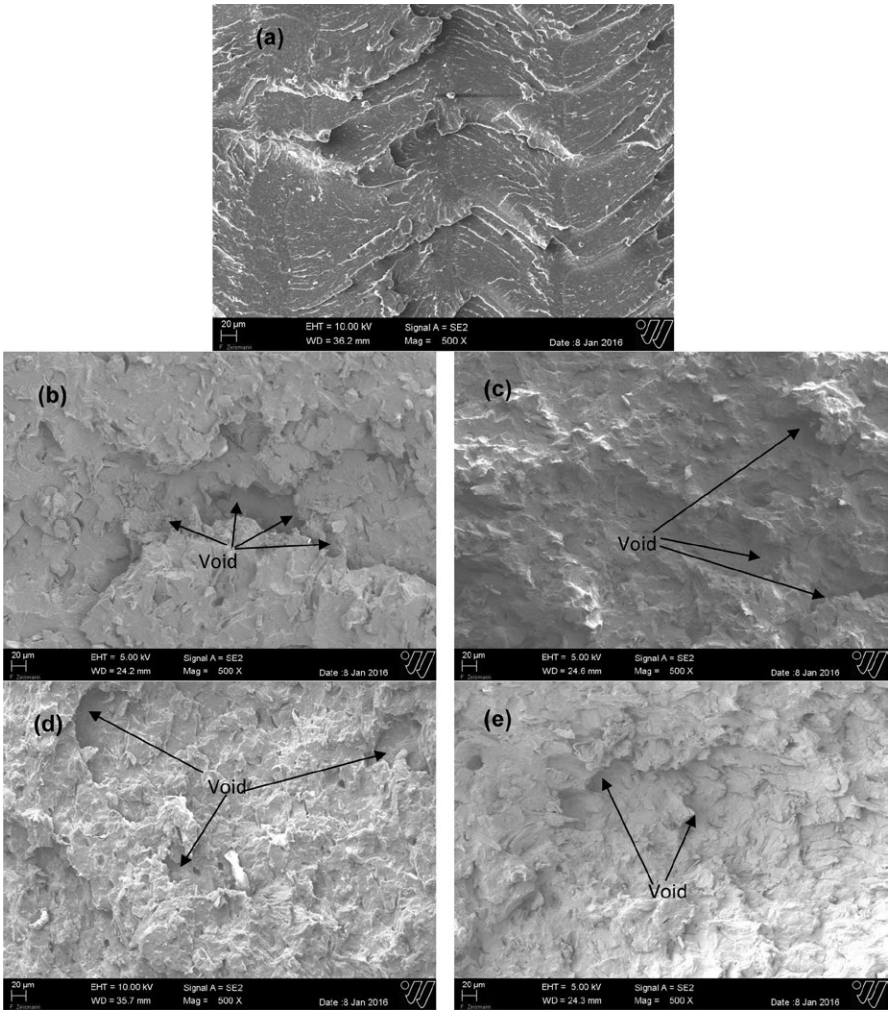

FIGURE 2 SEM of the fractured surface of neat PA (a) and different composites: (b) PA20F, (c) PA30F, (d) PA30F2VA, and (e) PA30F5VA

increases with the particle size for a fixed amount of loading. In addition, for the thermoplastic composites materials, the toughness is also influenced by the particle size and size distribution during impact loading.[23] For micro-sized fiber-based composites, it is expected to have better toughness with increasing size of particles.[24] This information

will be helpful for future investigation, while variation of the properties in respect to fiber length will be one of the significant scopes.

The surface of the fractured samples of the composites was observed by the SEM. The surface of PA, PA20F, PA30F, PA30F2VA, and PA30F5VA is illustrated in Figure 2a–e, respectively. The featureless image of PA can be seen in Figure 2a, whereas relatively rougher image can be observed in fiber and VA-based composites (Figure 2b–e). In the case of 20 wt.% fiber and 30 wt.% fiber-based samples, it is clear that the MCC fibers are visible like whisker, which create a microfibrillar structure and dispersed in the polymer matrix. The structure shows some voids and looks like a 3D network, which is thought to be the outcome of the melt rheological manufacturing technique.[25] On the other hand, using 2.0 wt.% VA improved the interfacial adhesion between the fibers and matrix, resulting a homogeneous distribution of the fibers with minimum or less void inside the matrix. The improved interactions are attributed due to the increasing number of hydrogen bonds between fibers and matrix in the presence of ethylene copolymer grafted with maleic anhydride.[19,26] For the case of 5.0 wt.% VA-based sample, the wettability of the fibers was increased, but voids were found due to high wettability and high flow of materials. Sometimes, the void can be formed due to the inadequate filler and fiber ratio, which was optimum for the case of PA30F2VA, as observed by the homogeneous distribution of the fibers in the presence of 2.0 wt.% VA. It can be predicted that the homogeneity of the components is ensured, if the fibers are distributed evenly with apparently no voids observed.

3.2 | Mechanical property analysis

The tensile properties of the composites are presented in Figure 3. Figure 3 represents tensile strength (TS) and tensile modulus (TM) of the samples, whereas Table 2 presents elongation at breaks (%). Significant changes were observed for the case of tensile modulus of the composites. The TM of the neat PA 6.10 was 2516 MPa, which was improved almost by 31% and 51% for the loading of 20 wt.% and 30 wt.% of the fiber, respectively. The TM of the composites was 3296 and 3802 MPa, respectively, using 20 and 30 wt.% loading of the fibers. In contrast, using VA did not improve the TM greatly. The TM of 2.0 wt.% of VA-based sample was 3893 MPa, whereas 5.0 wt.% of VA-based sample showed decreased TM of 3601 MPa. The excess amount of VA decreased the stiffness of the composites which resulted in decreased TM.

The neat PA showed the TS of 61.9 MPa, whereas 20 and 30 wt.% fiber-loaded sample showed the value of 58.8 and 62.3 MPa, respectively. The lower TS value at 20 wt.% fiber loading implied the inadequate stress transfer which was recovered at 30 wt.% fiber loading. Further, using 2.0 wt.% of VA improved the value to 63.1 MPa, which was again

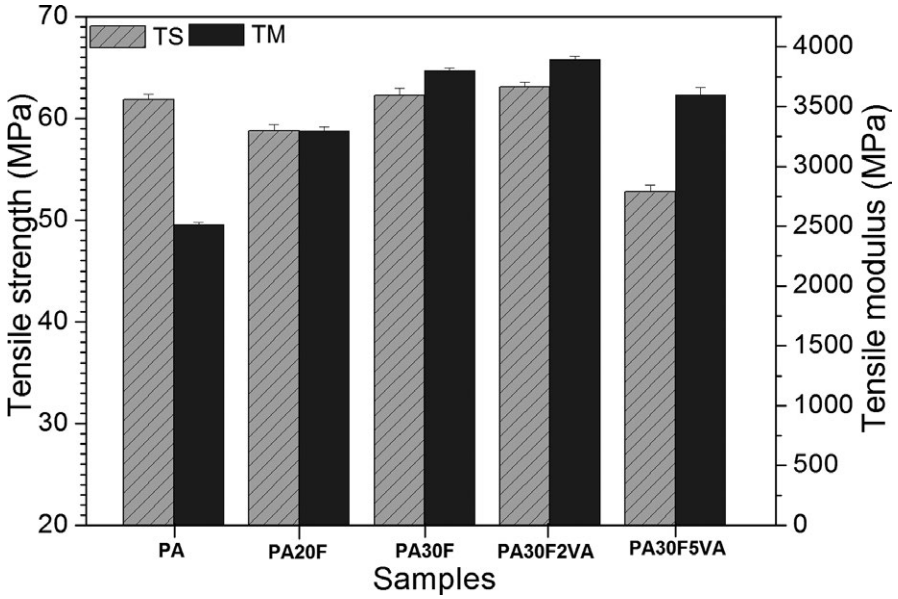

FIGURE 3 Tensile strength (MPa) and tensile modulus (MPa) of neat PA and different composites

TABLE 2 Elongation at break (%) and crystallinity (%) of different samples

Property	PA	PA20F	PA30F	PA30F2VA	PA30F5VA
Elongation at break (%)	28	3.5	2.6	3.4	2.6
Crystallinity (%)	26.7	24.5	19.0	19.2	19.3

decreased to much lower value of 52.8 MPa, at 5.0 wt.% of VA-based composites for 30 wt.% of fiber loading. The presence of higher amount of VA increased the stiffness of the composites. Therefore, the TS was found to be lower compared to other sample with 2.0 wt.% of VA.

The elongation at break (%) of the samples is listed in Table 2. From the table, it can be seen that the neat PA was a relatively tough material as reflected by the highest percentage (28%) of elongation at break. Using fibers (20 and 30 wt.%) and VA (2.0 and 5.0 wt.%) reduced the value by 90%–87%. The elongation at break % was recorded for the composites within a range of 2.6%–3.5%.

The impact strength (IS) of neat PA and different composites are graphically represented in Figure 4. The neat PA showed IS of 1.5 J/m^2, which was increased by almost 33% (2.0 J/m^2) due to the loading of 20 wt.% of fibers. Further, loading at 30 wt.%, the IS was improved to 2.3 J/m^2. On the other hand, using 2.0 wt.% of VA improved the IS almost by 100% (3.0 J/m^2), whereas 5.0 wt.% of VA enhanced it to the maximum value of 3.8 J/m^2. The coupling agent acts as a bridge between fiber and PA which improved the IS of the PA composite.[27,28] The standard deviation of the IS of PA, PA20F, PA30F, PA30F2VA, and PA30F5VA was found to be 0.469, 0.44, 0.202, 0.673, and 0.405, respectively. The standard deviations for the IS were high, and the data points were spread out of the range. The high differences were noticed due to the uneven or evenly distribution of the fibers for the same batch of different samples.

3.3 | Dynamic thermomechanical property analysis

A dual cantilever method was used for the dynamic thermomechanical property analysis. The effect of temperature, cellulose fiber content, and amount of VA was evaluated in terms of storage modulus, loss modulus, and tan delta. Figures 5, 6, and 7 represent the temperature vs. storage modulus (E'), temperature vs. loss modulus (E''), and temperature vs. loss tan delta (δ), respectively. It is known that different polymeric samples have different temperature dependence. Therefore, this test was carried out to understand the mechanical behavior of the polymer composites, while they are subjected to different temperatures rather than room temperature.

From the Figure 5, it can be seen that the neat PA shows a typical combination of glassy, glass transition, and rubbery properties. In the glassy state, the storage modulus did not change much below the temperature of 20°C. After that temperature, it started decreasing because of high percentage of crystallinity and the rate was found increasing due to the polymeric chain mobility and high viscosity.[29,30] The

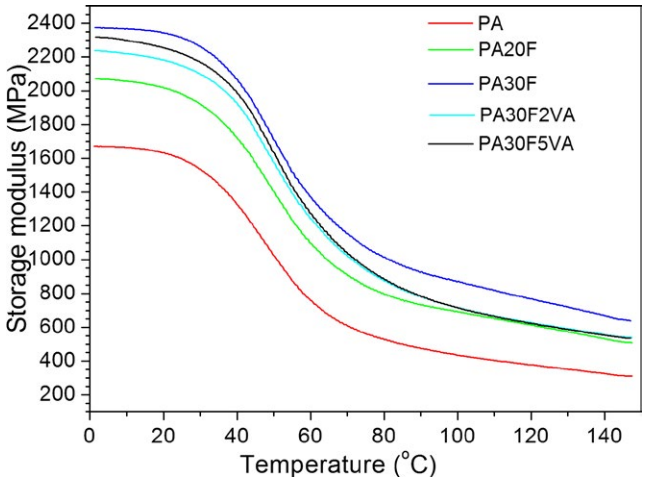

FIGURE 5 Storage modulus (MPa) of neat PA and different composites

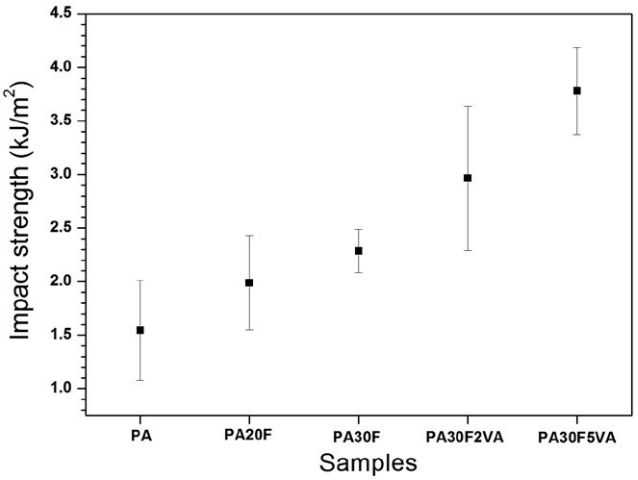

FIGURE 4 Impact strength (kJ/m^2) of neat PA and different composites

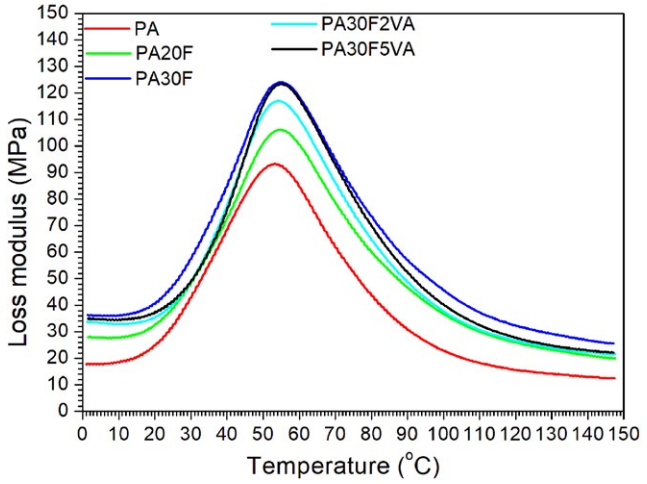

FIGURE 6 Loss modulus (MPa) of neat PA and different composites

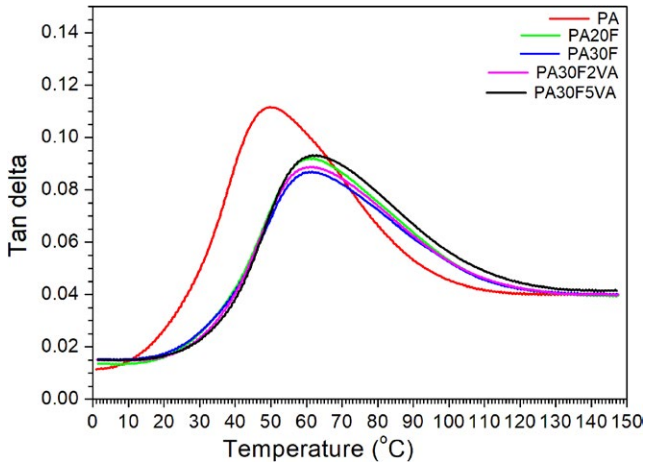

FIGURE 7 Tan delta of neat PA and different composites

decreasing was continued till the rubbery region around or after 120°C. As for comparison, from the Figure 5, it is clear that the storage modulus was found to be increased for all the composites.[31] In terms of fiber content, the storage modulus was found to be higher for 30 wt.% fiber loading compared to 20 wt.% of loading. The amount of VA content had a little effect on storage modulus. The values were close to each other, although 5.0 wt.% of VA content improved the storage modulus compared to 2.0 wt.% of VA-based composite. The storage modulus found to be decreased after adding filler for 30 wt.% of fiber-based composites. This is probably due to the low thermal stability of VA. The significant improvement of storage modulus was observed for all the composites after 100°C.

The curves for mechanical loss factor of different composites are presented in Figures 6 and 7. The peak temperature (Tan δ_{max}) for all the composites is presented in Table 3. From these data, the information for energy dissipation and glass transition temperature (T_g) of the composites can be predicted. The highest value of Tan δ_{max} was obtained as 11.36×10^{-2} for the case of neat PA. The highest value obtained for the loading of 20 and 30 wt.% of fibers was 9.21×10^{-2} and 8.63×10^{-2}, respectively. The higher value at higher loading indicates the strengthening effect due to fiber dispersion. The more fiber loading, the more contact area between fiber and matrix, which increased the total contact area and overall performance of the composites. On the other hand, 2.0 and 5.0 wt.% of VA containing samples showed the Tan δ_{max} value of 8.89×10^{-2} and $9.37 \times 10^{-2,}$ respectively. The imperfection in the elasticity can be measured using these values. From the figure, it is also obvious that the T_g values for the composites shifted to higher temperature, indicating the slower molecular mobility of the polymer matrix.

TABLE 3 The peak temperatures of loss modulus and tan delta

Material	Temperature Peak Tan Delta (°C)	Temperature Peak Loss Modulus (°C)
PA	50.0	53.3
PA20F	60.3	54.2
PA30F	60.2	54.4
PA30F2VA	60.4	52.3
PA30F5VA	61.3	53.1

3.4 | Structural properties

The XRD patterns of PA, PA20F, PA30F, PA30F2VA, and PA30F5VA are represented in Figure 8. It was found that PA, PA20F, and PA30F showed two apparent peaks at around 20.8° and 22.45° due to the presence of both γ and α phase crystallites in PA. The d-spacing for those peaks was found to be 0.44 and 0.39 nm, respectively. The presence of any peaks in the XRD spectra indicates the presence of some multilayer materials along with the cellulose fibers. The presence of VA shifted the peak from 22.45° to 23.07° and 23.89°, respectively, for 2.0 and 5.0 wt.% of loading. On the other hand, the presence of fibers inside PA showed two additional peaks at around 27.8° and 29.84°.

3.5 | Thermal properties

The TGA and DTG thermograms of various samples are shown in Figure 9a and b, respectively. Referring to the Figure 9a, weight (%) vs. temperature (°C) curve of PA showed that the onset degradation temperature was found to be 410°C. On the other hand, the incorporation of fiber (20 wt.%) showed a two-step degradation comprises with onset degradation temperature 300 and 391°C, respectively. The higher amount of fiber (30 wt.%) loading decreased to the onset degradation

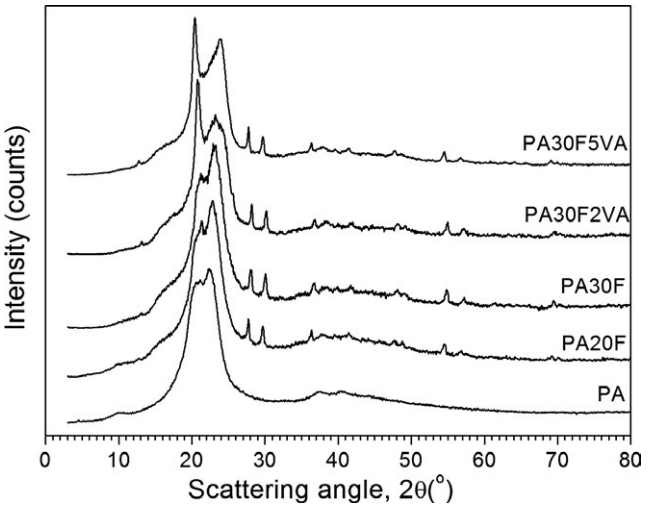

FIGURE 8 XRD diffractograms of different samples

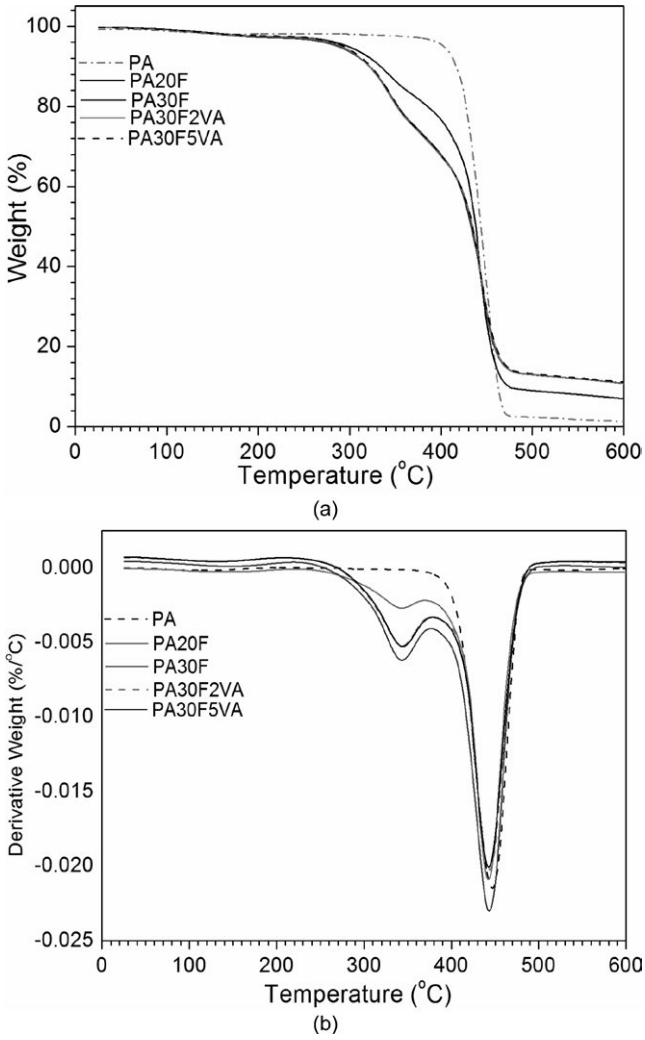

FIGURE 9 TGA thermograms of different samples: (a) weight (%) vs. temp. (°C) and (b) deriv. weight (%/°C) vs. temp. (°C)

temperature slightly. Apparently, no changes were observed due to the variation of VA amount and loading. The residues were found to be 1.8%, 7.1%, and 11.6% for the case of PA, 20 and 30 wt.% of fiber-based composites, respectively. Thus, the onset degradation temperature was decreased as the fiber loading increased. It was noticed that around 50% of mass loss was occurred near the temperature of 450°C. Figure 10b shows derivative weight (%/°C) vs. temperature (°C) of the samples. The T_{max1} was found to be 442°C, 443°C, and 448°C for the case of PA, fiber (20 and 30 wt.%), and VA(2.0 and 5.0 wt.%)-based composites. The differences measured are relatively small, and therefore, the potential effect of sample-to-sample variability cannot be ignored when differentiating these materials based on thermal properties alone. The T_{max2} was found to be absent for PA. The melting behavior of the samples was investigated via differential scanning calorimetry analysis. Figure 10 shows the melting behavior of the samples. The melting point of PA was found to be 226°C, which was decreased to 224°C after the incorporation of fibers. Further,

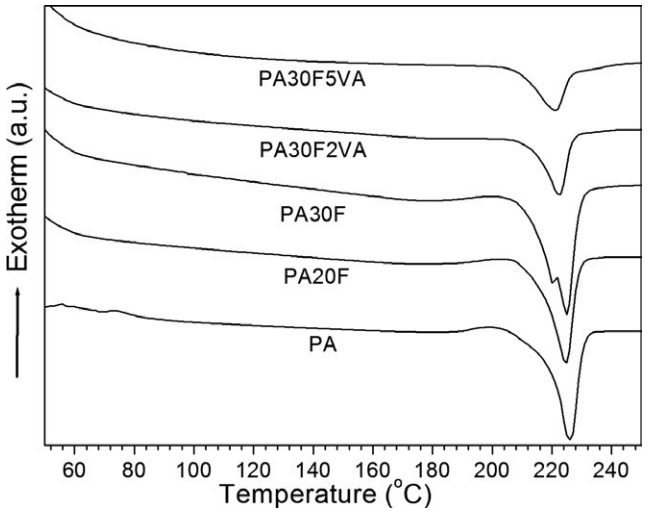

FIGURE 10 DSC thermograms of different samples

the addition of 2.0 wt.% of VA lower the melting point to 222°C, which was decreased more by 2°C, in the presence of 5.0 wt.% of VA. The crystallinity of PA was found to be 26.7%, which was found to be decreased with the inclusion of fibers.[18] The crystallinity was found to be 24.5% and 19.0% for the case of 20 wt.% and 30 wt.% of fiber loading. The melting points of the composites were decreased because of low crystallinity of the PA. No significant changes were observed for the using of coupling agent.

4 | CONCLUSION

The PA-based composites were prepared by reinforcing with microcrystalline cellulose in the presence of an impact modifier, VA, using extrusion and injection molding techniques. The fiber loading was considered as 20 and 30 wt.%. The coupling agent (VA) was varied (2.0 and 5.0 wt.%) for 30 wt.% fiber loading. The effects of the incorporation of microcrystalline cellulose and VA were analyzed in terms of mechanical, thermal, structural, morphological, and dynamic thermomechanical properties of the composites. It was found that the mechanical and thermomechanical properties of the composites were improved at 30 wt.% of fiber loading, whereas variation of coupling agent changes the properties slightly. From the thermodynamic analysis, it was also clear that the storage modulus was improved due to the higher amount of fiber loading. The DSC results showed that the incorporation of fibers and VA decreased the melting temperature which was even lower than neat PA.

ACKNOWLEDGMENT

The authors would like to thank the Hessen State Ministry of Higher Education, Research and the Arts-Initiative for

the Development of Scientific and Economic Excellence (LOEWE) for the financial support of the special research project "Safer Materials." Furthermore, the authors would like to thank the companies EVONIK industries and J. RETTENMAIER & SOHNE GmbH + Co KG for providing materials for this investigation.

ORCID

Muhammad Remanul Islam http://orcid.org/0000-0002-1714-6642

REFERENCES

[1] L.-Y. Chen, W. Li-Ping, H.-L. Zhang, Y.-B. Gao, J.-G. Gai, *Adv. Polym. Technol.* **2018**, *135*, 8 https://doi.org/10.1002/app.45891.
[2] B. S. Mbuli, S. D. Mhlanga, B. B. Mamba, E. N. Nxumalo, *Adv. Polym. Technol.* **2017**, *36*, 249 https://doi.org/10.1002/adv.21720.
[3] D. Battegazzore, J. Alongi, G. Fontaine, A. Frache, S. Bourbigot, G. Malucelli, *RSC Adv.* **2015**, *5*, 39424.
[4] D. A. Ruehle, C. Perbix, M. Castañeda, J. R. Dorgan, V. Mittal, P. Halley, D. Martin, *Polym.* **2013**, *54*, 6961.
[5] F. Xiuwei, L. Xiaohong, Y. Laigui, Z. Zhijun, *J. Appl. Polym. Sci.* **2010**, *115*, 3339.
[6] M. R. Islam, N. Isa, A. N. Yahaya, M. D. H. Beg, R. M. Yunus, *Adv. Polym. Technol.* **2017**, 1. https://doi.org/10.1002/adv.21823.
[7] M. A. S. A. Samir, F. Alloin, A. Dufresne, *Biomacromol* **2005**, *6*, 612.
[8] J. Chen, D. J. Gardner, *Polym. Compos.* **2008**, *29*, 372.
[9] R. Jacobson, D. Caulfield, K. Sears, J. Underwood, Sixth International Conference on Woodfiber/Plastic Composites, WI, **2002**, pp. 127–133. Madison
[10] J. O. Akindoyo, M. D. H. Beg, S. Ghazali, M. R. Islam, A. A. Mamun, *Polym. Plast. Technol. Eng.* **2015**, *54*, 42784.
[11] M. R. Islam, A. Gupta, M. Rivai, M. D. H. Beg, *J. Appl. Polym. Sci.* **2016**, *133*, 978.
[12] D. Battegazzore, S. Bocchini, J. Alongi, A. Frache, F. Marino, *Cellulose* **2014**, *21*, 1813.
[13] M. Feldmann, A. K. Bledzki, *Compos. Sci. Technol.* **2014**, *100*, 113.
[14] B. Wielage, T. Lampke, G. Marx, K. Nestler, D. Starke, *Thermochim. Acta* **1999**, *337*, 169.
[15] M. Maskavs, M. Kalnins, S. Reihmane, M. Laka, S. Chernyavskaya, *Mech. Compos. Mater.* **1999**, *35*, 55.
[16] A. Maskavs, M. Kalnins, M. Laka, S. Chernyavskaya, *Mech. Compos. Mater.* **2001**, *37*, 259.
[17] D. M. Panaitescu, P. V. Notingher, M. Ghiurea, F. Ciuprina, H. Paven, M. Iorga, D. Florea, *J. Opt. Elec. Adv. Mater.* **2007**, *9*, 2524.
[18] M. A. S. Azizi Samir, F. Alloin, J.-Y. Sanchez, A. Dufresne, *Polym.* **2004**, *45*, 4149.
[19] M. R. Islam, M. D. H. Beg, A. Gupta, *J. Thermoplast. Compos. Mater.* **2012**, *27*, 909.
[20] Q. Wu, X. Liu, L. A. Berglund, *Macromol. Rapid Commun.* **2001**, *22*, 1438.
[21] J. M. Lunt, J. B. Shortall, *Plast. Rubber Process.* **1979**, *4*, 108.
[22] S. Y. Fu, X. Q. Feng, B. Lauke, Y. W. Mai, *Composites Part B.* **2008**, *39*, 933.
[23] Y. Nakamura, M. Yamaguchi, *Polymer* **1992**, *33*, 3415.
[24] Z. Bartczak, A. S. Argon, R. E. Cohen, *Polymer* **1999**, *40*, 1247.
[25] S. K. Rahimi, J. U. Otaigbe, *Polym. Eng. Sci.* **2006**, *56*, 1045.
[26] J. K. Fink, Reactive Polymers Fundamentals and Applications A concise guide to industrial polymers, 2nd ed., Elsevier Science & Technology, Oxford, UK, **2013**.
[27] K. L. Pickering, M. G. Aruan Efendy, T. M. Le, *Compos. A* **2016**, *83*, 98.
[28] E. Franco-Marquès, J. A. Méndez, M. A. Pèlach, F. Vilaseca, J. Bayer, P. Mutjé, *Chem. Eng. J.* **2011**, *166*, 1170.
[29] H.-S. Kim, H.-S. Yang, H.-J. Kim, B.-J. Lee, T.-S. Hwang, *J. Therm. Anal. Calorim.* **2005**, *81*, 299.
[30] H.-S. Kim, S. Kim, H.-J. Kim, H.-S. Yang, *Thermochim. Acta* **2006**, *451*, 181.
[31] A. P. Mathew, K. Oksman, M. M. Sain, *J. Appl. Polym. Sci.* **2005**, *97*, 2014.

How to cite this article: Beg MDH, Islam MR, Mamun AA, Heim H-P, Feldmann M, Akindoyo JO. Characterization of polyamide 6.10 composites incorporated with microcrystalline cellulose fiber: Effects of fiber loading and impact modifier. *Adv Polym Technol*. 2018;37:3412–3420. https://doi.org/10.1002/adv.22125